

Creep Bending and Buckling of Nonlinear Viscoelastic Columns with Applications to CANDU Fuel Sheaths*

S. D. Yu and X. Zhang

Department of Mechanical and Industrial Engineering, Ryerson University, Toronto, Ontario, Canada M5B 2K3

ABSTRACT

This paper presents a procedure for two-dimensional creep bending of beams or columns made linear or nonlinear visco-elastic materials. The procedure is developed using higher-order beam finite elements in the space domain and the incremental method in the time domain. Simulation results indicate that the procedure is accurate and convergent for linear and nonlinear viscoelastic beams. The procedure presented in this paper has been extended to three-dimensional creep bending and implemented into the BOW[#] code for elastic-creep assessment of a string of CANDU nuclear fuel bundles.

INTRODUCTION

A standard CANDU[®]6 fuel bundle stays in a reactor for about six months before being discharged at an exit burnup of about 260 MWh/kgU. During the reactor life, individual fuel elements experience considerable amount of creep at elevated temperatures, which may potentially cause contact with the pressure at undesirable locations, interfere with bundle removal at the end of life, etc. Quantification of creep bending and buckling is important in new fuel design. The elasto-creep deformations of CANDU fuel are usually assessed using the BOW code in the Canadian nuclear industry [1]-[3].

This paper presents the most recent research work in developing an efficient and accurate algorithm for modeling elasto-creep bending of CANDU fuel elements. For compatibility with the BOW code, the elasto-creep algorithm is developed within the framework of beam finite element method. In handling the axial variations of strains/stresses within a beam finite element due to bending, a four-point Gaussian quadrature scheme is adopted for determining the creep loads. At each axial Gaussian point, the beam cross section is divided into many 9-node lagrangian elements or cells for computing the creep moments and modeling accurately the curvilinear boundaries of the cross section; the 4 by 4 Gaussian quadrature scheme is employed to evaluate the creep-induced bending moments within each 9-node lagrangian element or cell.

Since creep is a very slow process, the inertial effect is neglected. As a result, equilibrium condition holds at any instant. The Galerkin principle may be used to establish a set of governing equations in terms of the total displacements and the classical beam bending theory. The so-obtained equations are nonlinear for nonlinear visco-elastic materials. Their solutions are obtained numerically using the finite difference method in the time domain.

MATHEMATICAL DESCRIPTION OF CREEP BENDING ALGORITHMS

Constitutive Equations

For a straight beam and the coordinates shown in Fig. 1, the total axial strain of a material point is sum of the elastic, initial, and thermal and creep components at any given time. It is written as

$$\varepsilon_z = \varepsilon_z^e + \varepsilon_z^0 + \varepsilon_z^h + \varepsilon_z^c \quad (1)$$

In dealing with elasto-creep deformations of materials such as Zircaloy, the creep strain rate at a given time is usually dependent on several state variables in an explicit manner. The correlations between the local creep strain rate and the set of state variables are termed as the creep laws, which are established through experiments. The state variables in a creep law may include stress and/or strain, temperature and neutron flux when dealing with creep of a nuclear component such as Zircaloy cladding. In general, the accumulated creep strain at a material point at time t may be written as

$$\varepsilon_z^c(t) = \int_0^t \dot{\varepsilon}_z^c(\tau; x, z) d\tau \quad (2)$$

where τ is the time integration variable. For a given creep law specific to a material, the elasto-creep deformations of beams made of such material, are dependent on loads and loading history. For a nonlinear creep law, it is difficult to obtain an analytical solution to the elasto-creep bending of a beam. In simulating creep bending, approximate numerical solutions are often sought.

* A computer code at Atomic Energy of Canada Ltd. for assessment of creep bowing of CANDU fuel bundles.

[®] CANDU is a registered trademark of Atomic Energy of Canada Ltd. (AECL).

Combining Eq. (1) and Eq. (2), according to Hooke' law, the constitutive equation for a uni-axial strain/stress problem may be written as

$$\sigma_z = E(\varepsilon_z - \varepsilon_z^0 - \varepsilon_z^{th}) - E \int_0^t \dot{\varepsilon}_z^c(\tau; x, z) d\tau \quad (3)$$

where E is the modulus of elasticity.

In this paper, the focus is on the development of a creep algorithm. The temperature in the beam is considered uniform. The axial thermal strain is simply a constant, or $\alpha\Delta T$, where α is the coefficient of thermal expansion, and ΔT is the temperature rise with reference to a reference (room) temperature.

For a slender beam, it may be assumed that the total lateral deformation obeys the Euler-Bernoulli beam theory without consideration of the transverse shear deformations. For the rectangular coordinates used, the total axial strain due to combined axial and bending deformations may be written as

$$\varepsilon_z = \frac{\partial w}{\partial z} - \frac{\partial^2 u}{\partial z^2} x \quad (4)$$

where u is the lateral deflection in the x direction; w is the axial deflection in the z direction.

Substituting Eq. (4) into Eq. (3), a preferred relationship between the stress and the deformations may be written as

$$\sigma_z = E \frac{\partial w}{\partial z} - E \frac{\partial^2 u}{\partial z^2} x + E \frac{\partial^2 u_0}{\partial z^2} x - E\alpha\Delta T - E \int_0^t \dot{\varepsilon}_z^c(\tau; x, z) d\tau \quad (5)$$

where u_0 is the initial lateral deflection in the x direction.

Two meaningful stress resultants may be obtained for the axial and lateral deformations of a fuel element. They are the axial force (positive for tension and negative for compression) and bending moments M_x (positive if consistent with the curvature). At an axial location, the three meaningful stress resultants may be obtained using the following expression

$$\begin{aligned} F_z &= \int_{A_i} \sigma_z dA = EA \frac{\partial w}{\partial z} - F_z^{th} - F_z^c \\ M_x &= - \int_{A_i} \sigma_z x dA = EI \frac{\partial^2 u}{\partial z^2} - M_x^0 - M_x^c \end{aligned} \quad (6)$$

where

$$F_z^{th} = \int_A E\alpha\Delta T dA, \quad F_z^c = E \int_0^t \left(\int_A \dot{\varepsilon}_z^c(\tau; x, z) dA \right) d\tau, \quad M_x^0 = EI \frac{\partial^2 u_0}{\partial z^2}, \quad M_x^c = - \int_0^t \left(\int_A E \dot{\varepsilon}_z^c(\tau; x, z) x dA \right) d\tau$$

Note that it is assumed in deriving Eq. (6) that the centroid of the cross section coincides with the z axis.

Equations of Equilibrium

To derive the governing differential equations for axial and lateral deformations of a beam, an infinitesimal element is cut out from a fuel element. For small deformations, the following two equilibrium conditions may be established

$$\begin{aligned} Q_x + \frac{\partial M_x}{\partial z} &= 0 \\ - \frac{\partial Q_x}{\partial z} - F_z \frac{\partial^2 u}{\partial z^2} - \frac{\partial F_z}{\partial z} \frac{\partial u}{\partial z} &= q_x + \sum_k P_{k,x} \delta(z - z_k) \end{aligned} \quad (7)$$

Solving the transverse shear force in terms of the bending moment, a single equation of equilibrium governing the beaming bending in the xoz plane may be written as

$$\frac{\partial^2 M_x}{\partial z^2} - F_z \frac{\partial^2 u}{\partial z^2} - \frac{\partial F_z}{\partial z} \frac{\partial u}{\partial z} = q_x + \sum_k P_{k,x} \delta(z - z_k) \quad (8)$$

In the axial direction, the equilibrium condition may be written as

$$- \frac{\partial F_z}{\partial z} = q_z + \sum_j F_{j,z} \delta(z - z_j) \quad (9)$$

In Eqs. (8) and (9), q_x and q_z are line intensities of distributed loads in the two coordinate directions; Q_x is the transverse shear force in the x direction; $P_{k,y}$ is transverse loads in the x direction; $\delta(z - z_k)$ are Dirac delta functions. In a CANDU reactor, line load q_x may be used to account for the gravitational effect; and q_z can be used to account for the distributed hydraulic drag effect. Concentrated vertical forces $P_{k,x}$ are used to account for the effect of lateral contact forces; and concentrated axial forces $F_{k,z}$ are used to account for the axial contact forces.

It is difficult to obtain an exact analytical solution to the elasto-creep problem of a beam because of the nonlinear constitutive equations and distributed axial forces. In addition, spacer pads and bearing pads attached to a fuel element also makes it impossible to seek an analytical solution. As a result, an approximate numerical solution is to be obtained using the the finite element method. To facilitate the subsequent finite element procedure, the following weak form of equilibrium equation may be obtained by multiplying Eq. (8) by u^* and Eq. (9) w^* , and adding the so-obtained equations together, and then integrating the with respect to z over the entire beam length

$$\begin{aligned} & \int_0^{l_e} \frac{\partial w^*}{\partial z} F_z dz - w F_z \Big|_0^{l_e} + \left[\int_0^{l_e} \frac{\partial^2 u^*}{\partial z^2} M_x + \frac{\partial u^*}{\partial z} F_z \frac{\partial u}{\partial z} \right] dz - u^* \left(Q_x + F_z \frac{\partial u}{\partial z} \right) \Big|_0^{l_e} - \frac{\partial u^*}{\partial z} M_x \Big|_0^{l_e} \\ & = \int_0^{l_e} w^* q_z dz + \sum_j w^* P_{j,z} \Big|_{z=z_j} + \int_0^{l_e} u^* q_x dz + \sum_k u^* Q_{k,x} \Big|_{z=z_k} \end{aligned} \quad (10)$$

Finite Element Procedure

To be able to capture the axial variations of creep loads for the nonlinear creep law, a three-node beam element is employed. The axial and lateral displacements within this beam finite element are determined from the shape functions and element nodal displacements as follows

$$w(\zeta) = [N_1][D_1]\{\bar{w}_e\}, u(\zeta) = [N_2][D_2]\{\bar{u}_e\} \quad 0 \leq \zeta \leq l_e \quad (11)$$

where shape function matrices, the element nodal displacement vectors and the element geometric matrices are defined as follows

$$\begin{aligned} [N_1] &= [1 \quad \zeta \quad \zeta^2] [N_2] = [1 \quad \zeta \quad \zeta^2 \quad \zeta^3 \quad \zeta^4 \quad \zeta^5] \\ \{\bar{w}_e\} &= \begin{Bmatrix} w_1 \\ w_2 \\ w_3 \end{Bmatrix}, \{\bar{u}_e\} = \begin{Bmatrix} u_1 \\ \theta_1 \\ u_2 \\ \theta_2 \\ u_3 \\ \theta_3 \end{Bmatrix}_e, [D_{e,1}] = \begin{bmatrix} 1 & 0 & 0 \\ -3 & 4 & -1 \\ l_e & l_e & l_e \\ 2 & -4 & 2 \\ l_e^2 & l_e^2 & l_e^2 \end{bmatrix}, [D_{e,2}] = \begin{bmatrix} 1 & 0 & 0 & 0 & 0 & 0 \\ 0 & 1 & 0 & 0 & 0 & 0 \\ -23 & -6 & 16 & -8 & 7 & -1 \\ l_e^2 & l_e & l_e^2 & l_e & l_e^2 & l_e \\ 66 & 13 & -32 & 32 & -34 & 5 \\ l_e^3 & l_e^2 & l_e^3 & l_e^2 & l_e^3 & l_e^2 \\ -68 & -12 & 16 & -40 & 52 & -8 \\ l_e^4 & l_e^3 & l_e^4 & l_e^3 & l_e^4 & l_e^3 \\ 24 & 4 & 0 & 16 & -24 & 4 \\ l_e^5 & l_e^4 & l_e^4 & l_e^5 & l_e^4 & l_e^4 \end{bmatrix} \end{aligned}$$

where $\theta = \frac{\partial u}{\partial z}$.

To derive the approximate equations of equilibrium from Eq. (10), the global arbitrary displacement fields, $u^*(z)$ and $w^*(z)$, are defined for each finite beam element with the help of the shape functions for true displacements in Eq. (11) and arbitrary element nodal displacement vectors as follows

$$w^*(\zeta) = [N_1][D_{e,1}]\{\bar{w}_e^*\}, u^*(\zeta) = [N_2][D_{e,2}]\{\bar{u}_e^*\}, \quad 0 \leq \zeta \leq l_e \quad (12)$$

Substituting Eqs. (11) and (12) in Eq. (10), and invoking the arbitrariness of $\{\bar{u}_e^*\}$ and $\{\bar{w}_e^*\}$, one obtains

$$\begin{aligned} & \sum_{e=1}^{N_e} \{\bar{w}_e^*\}^T [D_{e,1}]^T \left\{ \int_0^{l_e} EA [N_1]^T [N_1] d\zeta [D_{e,1}] \{\bar{w}_e^*\} - \int_0^{l_e} [N_1]^T (F_z^{th} + F_z^c) d\zeta \right\} \\ & \sum_{e=1}^{N_e} \{\bar{u}_e^*\}^T [D_{e,2}]^T \left\{ \int_0^{l_e} (EI [N_2]^T [N_2] + F_z [N_2]^T [N_2]) d\zeta [D_{e,2}] \{\bar{u}_e^*\} - \int_0^{l_e} [N_2]^T (M_x^0 + M_x^c) d\zeta \right\} \\ & = \sum_{e=1}^{N_e} \{\bar{w}_e^*\}^T [D_{e,1}]^T \int_0^{l_e} [N_1]^T q_z d\zeta + \sum_{e \in e_j} \{\bar{w}_e^*\}^T [D_{e,1}]^T [N_1(\zeta_j)]^T F_{j,z} \\ & \quad + \sum_{e=1}^{N_e} \{\bar{u}_e^*\}^T [D_{e,2}]^T \int_0^{l_e} [N_2]^T q_x d\zeta + \sum_{e \in e_k} \{\bar{u}_e^*\}^T [D_{e,2}]^T [N_2(\zeta_k)]^T P_{k,x} \end{aligned} \quad (13)$$

where e_k is the finite element containing lateral load $Q_{k,x}$; e_j is the finite element enclosing axial lateral load $P_{j,z}$; ζ_k is the local axial coordinate for z_k in element e_k ; ζ_j is the local axial coordinate for z_j in element e_j .

Finally, to assemble the component equations for a fuel element, the element nodal displacement vectors are related to the component displacement vector through the following transformation matrix

$$\begin{aligned}\{\bar{w}_e\} &= [T_{e \rightarrow g}^{(w)}] \{\bar{w}\}, \{\bar{u}_e\} = [T_{e \rightarrow g}^{(u)}] \{\bar{u}\} \\ \{\bar{w}_e^*\} &= [T_{e \rightarrow g}^{(w)}] \{\bar{w}^*\}, \{\bar{u}_e^*\} = [T_{e \rightarrow g}^{(u)}] \{\bar{u}^*\}\end{aligned}\quad (14)$$

Introducing the transformations in Eq. (14) into Eq. (13), one obtains the following equations of equilibrium

$$\begin{aligned}[K_w] \{\bar{w}\} &= \{\bar{F}\} + \{\bar{F}\}^{(th)} + \{\bar{F}\}^{(c)} \\ [K_u] \{\bar{u}\} &= \{\bar{P}\} + \{\bar{P}\}^{(0)} + \{\bar{P}\}^{(c)}\end{aligned}\quad (15)$$

where

$$\begin{aligned}[K_w] &= \sum_{e=1}^{N_s} [T_{e \rightarrow g}^{(w)}]^T [D_{e,1}]^T \left\{ \int_0^l EA [N_1]^T [N_1] d\zeta \right\} [D_1] [T_{e \rightarrow g}^{(w)}] \\ [K_u] &= \sum_{e=1}^{N_s} [T_{e \rightarrow g}^{(u)}]^T [D_{e,2}]^T \left\{ \int_0^l EI [N_2]^T [N_2] d\zeta + \int_0^l F_z [N_2]^T [N_2] d\zeta \right\} [D_{2,2}] [T_{e \rightarrow g}^{(u)}] \\ \{\bar{F}\}^{(th,c)} &= \sum_{e=1}^{N_s} [T_{e \rightarrow g}^{(w)}]^T [D_{e,1}]^T \int_0^l [N_1]^T (F_z^{th}, F_z^c) d\zeta \\ \{\bar{P}\}^{(0,c)} &= \sum_{e=1}^{N_s} [T_{e \rightarrow g}^{(u)}]^T [D_{e,2}]^T \int_0^l [N_2]^T (M_x^0, M_x^c) d\zeta \\ \{\bar{F}\} &= \sum_{e=1}^{N_s} [T_{e \rightarrow g}^{(w)}]^T [D_{e,1}]^T \int_0^l [N_1]^T q_z d\zeta + \sum_{e \in e_j} [T_{e \rightarrow g}^{(w)}]^T [D_{e,1}]^T [N_1(\zeta_j)]^T F_{j,z} \\ \{\bar{P}\} &= \sum_{e=1}^{N_s} [T_{e \rightarrow g}^{(u)}]^T [D_{e,2}]^T \int_0^l [N_2]^T q_x d\zeta + \sum_{e \in e_k} [T_{e \rightarrow g}^{(u)}]^T [D_{e,2}]^T [N_2(\zeta_k)]^T P_{k,x}\end{aligned}$$

It is noted that the two sets of equations in Eq. **Error! Reference source not found.** are not directly coupled. A solution to the two sets of equations may be obtained separately. However, to account for the effect of the axial force on the lateral deformations, the first set of equations must be solved first.

Handling Creep-Induced Deformations

For metals such as Zircaloy at elevated temperatures, the local creep rate may vary in a highly non-linear manner with the local stress, local strain, temperature, etc. As a result, both sets of equations in Eq. **Error! Reference source not found.** are nonlinear. To obtain a time-dependent solution, an incremental approach is adopted in the time domain. In an elasto-creep analysis, the elastic analysis is first conducted. At the end of the elastic step, an initial local stress and strain field may be established. This initial stress/strain field may be used to evaluate the creep rate in the next small time interval. A set of hierarchical equations may be written as

$$\begin{aligned}[K_w]_{j-1} \{\bar{w}\}_i &= \{\bar{F}\}_{j-1} + \{\bar{F}\}_{j-1}^{(th)} + \{\bar{F}\}_{j-1}^{(c)} \\ [K_u]_{j-1} \{\bar{u}\}_i &= \{\bar{P}\}_{j-1} + \{\bar{P}\}_{j-1}^{(0)} + \{\bar{P}\}_{j-1}^{(c)}\end{aligned}\quad (16)$$

where subscript $j-1$ and i indicates that the quantities are evaluated at times $t = t_{j-1}$ and $t = t_i$.

The creep process in the subsequent time interval is very complex; assumptions must be made in order to obtain an approximate solution of good accuracy. When a reasonably small time increment is used, it may be assumed that in the $\Delta t_i = t_i - t_{j-1}$ duration, the creep strain rate is constant and equal to that at $t = t_{j-1}$. During the entire interval, the creep strain is considered varying in a linear manner. Since creep process is a slow process, at any instant the static equilibrium equation holds. At the end of the previous time interval, the creep loads $\{\bar{P}\}_{j-1}^{(c)}$ and $\{\bar{F}\}_{j-1}^{(c)}$ may be developed from the constant creep strain rate assumption. The distributed creep loads within a beam finite element at time t may be determined from

$$F_z^c(\zeta, t) = \Delta t_i \int_A E \dot{\epsilon}_{i-1} dA, \quad M_x^c(\zeta, t) = -\Delta t_i \int_A E \dot{\epsilon}_{i-1} x dA \quad \text{for } 0 \leq \zeta \leq l_e, t_{j-1} \leq t \leq t_i \quad (17)$$

The nodal creep load vectors for a beam element may be obtained using

$$\begin{aligned}\{\bar{F}_w\}_{j-1}^{(c)} &= \Delta t_i \sum_{e=1}^{N_s} [T_{e \rightarrow g}^{(w)}]^T [D_{e,1}]^T \int_0^l \int_{A_e} [N_1]^T E \dot{\epsilon}_{i-1} dA d\zeta \\ \{\bar{P}_u\}_{j-1}^{(c)} &= -\Delta t_i \sum_{e=1}^{N_s} [T_{e \rightarrow g}^{(u)}]^T [D_{e,2}]^T \int_0^l \int_{A_e} [N_2]^T E \dot{\epsilon}_{i-1} x dA d\zeta\end{aligned}\quad (18)$$

To determine the above volume integrals accurately, a numerical quadrature scheme is developed. To evaluate the area integrals at a cross section, the beam finite element is divided into a desired number of cells having nine nodes in order to capture the curvilinear boundaries. For the two example cross sections shown in Fig. 1, a total of 64 nine-node lagrangian cells are employed. A detailed view of the 64 cells is illustrated in Fig. 2. The Within each cell, a 4×4 Gaussian quadrature is used to calculate the creep loads. The creep load vector may be determined from the following equations

$$\int_0^L \int_A [N_2]^T E \dot{\epsilon}_{i-1} x dA d\zeta = \sum_{k=1}^4 w_k [N_2(\zeta_k)]^T m_{x,k}^{(c)} \quad (19)$$

$$m_{x,k}^{(c)} = \int_A (E \dot{\epsilon}_{i-1})_{\zeta=\zeta_k} x dA$$

where w_k is the weights associated with the 4-point Gaussian quadrature [4]; ζ_k is the axial coordinate of k -th Gaussian point.

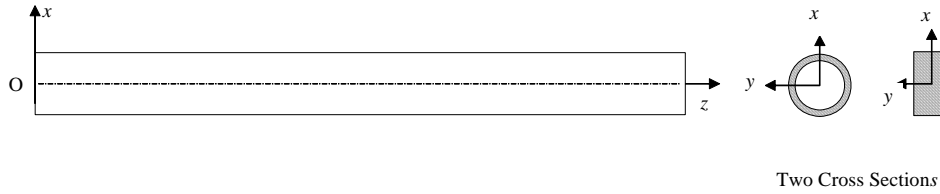


Fig. 1 A straight and slender nonlinear visco-elastic beam

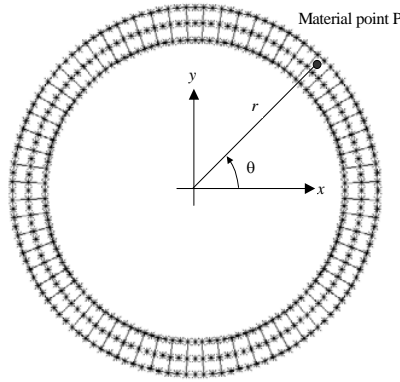


Fig. 2 The 9-node curvilinear lagrangian cells used for creep moment calculations

NUMERICAL RESULTS

Numerical results were first obtained for a simply supported beam of hollow circular cross section (outer diameter 11.5 mm, inner diameter 10.8 mm, length 495.06 mm). The beam is subjected to a constant compressive axial load, $F = 300$ N. The initial stress-free deformation is $\delta_0 \sin(\pi z / L)$, where $\delta_0 = 0.5$ mm. For linear visco-elastic material whose creep strain rate is $\dot{\epsilon}_z^c = \sigma_z / E_c$, an analytical solution for lateral deflection may be written as [5]

$$u(z) = \frac{\delta_0}{1 - F / F_{cr}} e^{\omega t} \sin(\pi z / L) \quad (20)$$

where $F_{cr} = EI(\pi/L)^2$, $\omega = (E / E_c)(F_{cr} / F - 1)$; E ($= 80.447$ GPa) is the modulus of elasticity; E_c ($= 1.49E18$ Pa·s) is the creep modulus. For convergence tests, the midspan stationary creep deformation of the beam at the end of 4800 hours after the application of the axial force are monitored. Numerical results given in Table 1 show that the algorithm converges rapidly with the number of beam finite elements used and at a slower rate with the time increment used. The solution converges to the exact value if more than two beam finite elements and a time increment of smaller than 3.75 hours are used. Comparisons between the two sets of results, shown in Fig. 3 and Fig. 4, indicate that there is excellent agreement between the analytical solution and the results obtained using the procedure described in this paper.

Table 1 Convergence Tests for a Linearly Visco-elastic Beam

Number of Beam Finite Elements Used	Time Increment (hours)					
	120	60	30	15	7.5	3.75
1	2.279	2.307	2.323	2.331	2.335	2.337
2	2.283	2.311	2.327	2.335	2.339	2.341
3	2.283	2.311	2.327	2.335	2.339	2.341
4	2.283	2.311	2.327	2.335	2.339	2.341
5	2.283	2.311	2.327	2.335	2.339	2.341
Exact	2.341	2.341	2.341	2.341	2.341	2.341

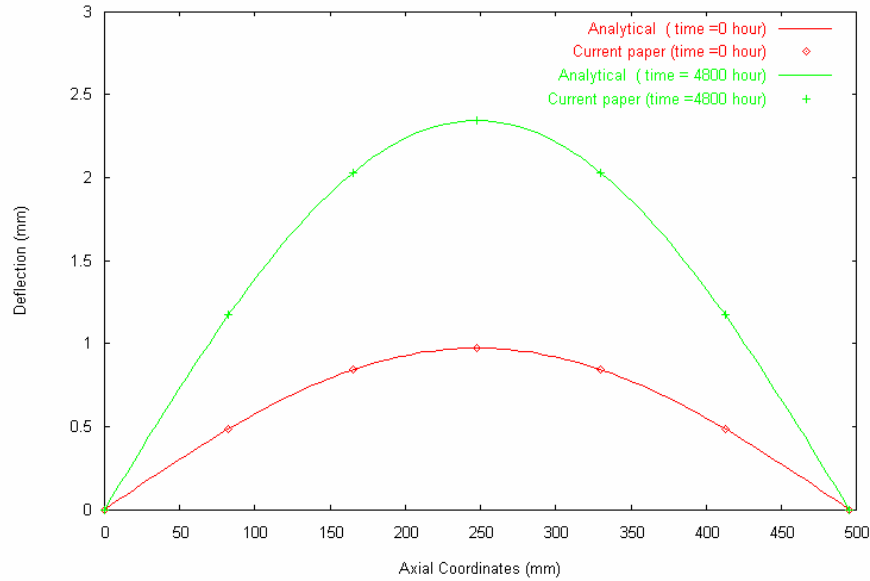


Fig. 3 Midspan Deflection vs. time

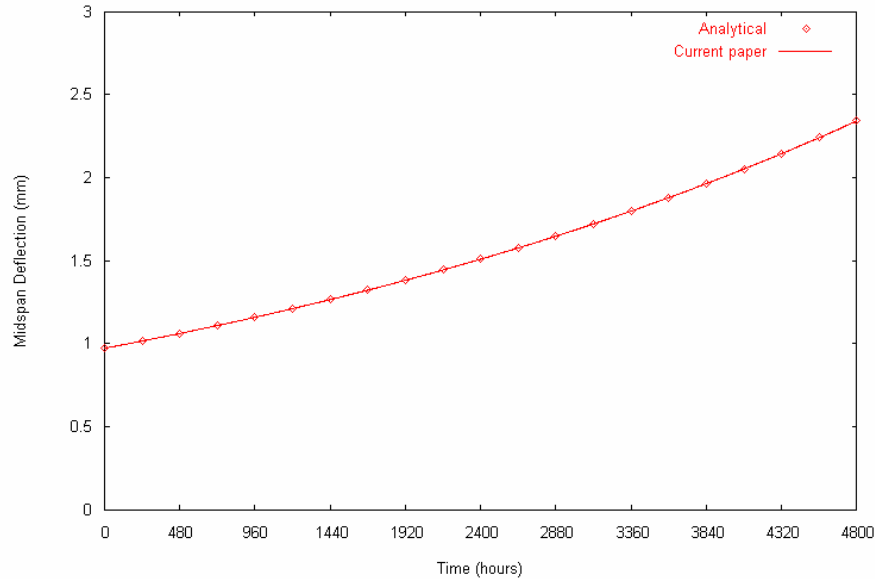


Fig. 4 Midspan deflections of a linear viscoelastic beam with vs. time

As a second example, a simply supported beam of square cross section (sides: 13.5 mm by 13 mm, length 495.06 mm) is studied. To compare with results available in the literature, the nonlinear viscoelastic material is assumed to obey the

following the creep law

$$\dot{\epsilon}_z^c = \lambda p t^{p-1} \sigma_z^m \quad (21)$$

The upper and lower bounds of creep bending of the simply supported beam obeying the above creep law were obtained analytically by Bleich [6]. For the purpose of evaluating convergence rates and verifying the simulation results, Bleich's upper and lower bounds were obtained for the following values of the parameters in Eq. (21): $p=1$,

$m=1$, $\lambda = 3.924 \times 10^{-33} \text{ Pa}^{-\frac{1}{3}}/\text{s}$. Value of Young's modulus used is 80.447 GPa. The stress-free initial deflection profile is sinusoidal $0.0292 \sin(\pi z/L)$ mm. The axial load is $F = 8000$ N, or 89.2% of the critical buckling load. Unlike the linear viscoelastic material, the distributions of creep-induced strains at a cross section are nonlinear, and change significantly with time as the structure experiences the creep deformations, as shown in Fig. 6 for the creep strain profiles at the midspan cross section at three different times. Results in Fig. 6 show that (i) the midspan deflections, normalized with respect to the beam cross section height, converge rapidly for time increments smaller than 0.1 hour; (ii) the converged solutions also lie between the lower and upper bounds established by Bleich [6]. The non-dimensional time, t' , is related to the actual time through the following relationship:

$$t' = \frac{3EA\lambda\sigma_0^3}{F_{cr} - F} t \quad (22)$$

where A is the cross sectional area of the beam. When the non-dimensional time approaches 3.25 or 60 hours (critical creep buckling time) after the application of the load, the beam deflection starts to increase dramatically with time. The beam cannot carry the load safely beyond the critical creep buckling time.

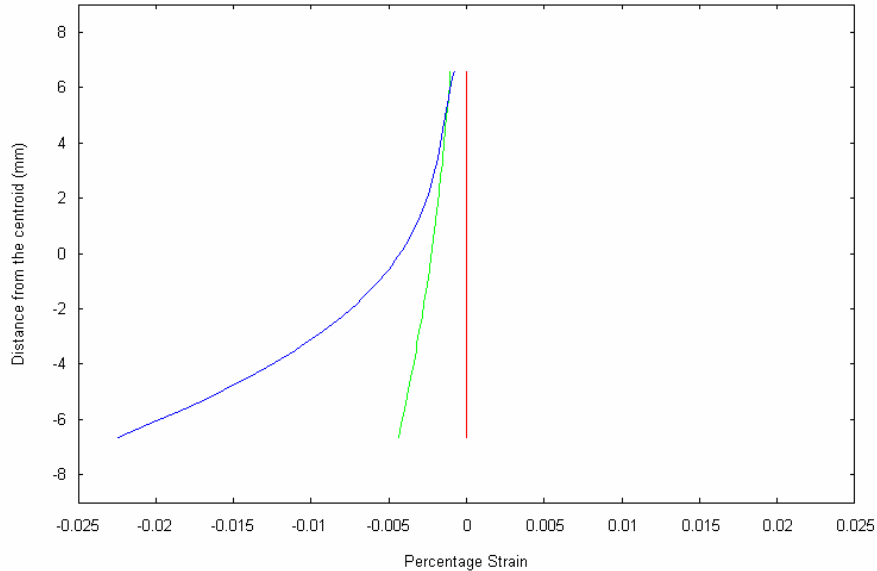


Fig. 5 Creep strain profiles at the midspan cross section at different times

CONCLUSIONS

A numerical procedure is developed in this paper to handle creep bending and creep buckling of nonlinear viscoelastic beams. Simulation results show that the procedure is accurate and convergent. The algorithm has been implemented into the BOW code for assessment of elasto-creep deformations of a string of fuel bundles.

ACKNOWLEDGEMENT

The authors would like to thank G. S. Xu and Z. Xu of AECL for many valuable suggestions and discussions during the preparation of this manuscript. The financial support from the Natural Sciences and Engineering Sciences (NSERC) and AECL through an NSERC Collaborative Research Grant is gratefully acknowledged.

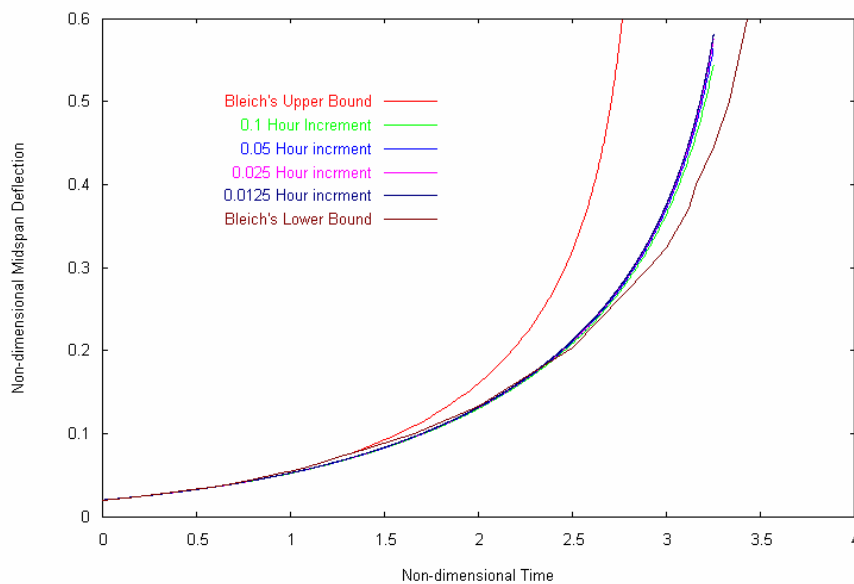


Fig. 6 Midspan Deflections vs. time for a nonlinear visco-elastic beam

REFERENCES

- [1] Veeder, J., and Schankula, M., "Bowling of Pelletized Fuel Elements: Theory and In-Reactor Experiments", *Nuclear Engineering and Design* 29, 1974, pp 167-179.
- [2] Tayal, M., "Modelling the Bending/Bowling of Composite Beams such as Nuclear Fuel: the BOW Code," *Nuclear Engineering and Design* 116, 1989, pp 149-159.
- [3] S.D. Yu, M. Tayal and Z. Xu, "Creep Bowling in CANDU Fuel: Modelling and Applications", *Proceeding of the Fifth International Conference on CANDU Fuel*, 1997, September-21-25, pp 364-375, Toronto, Canada.
- [4] K-J. Bathe, *Finite Element Procedure*, Prentice Hall, 1997.
- [5] Xu, G.S., Yu, S.D., Tayal, M., and Xu, Z., "BOW: Comparisons of Creep Calculations with Analytical Solutions," *Proc. of the 6th Int. Conf. on Simulation Methods in Nuclear Eng.*, Montreal, October 13-15, 2004.
- [6] Bleich, H. H. and Dillon, O.W., "Nonlinear Creep Deformations of Columns of Rectangular Cross Section," *Journal of Applied Mechanics*, 1959, pp 517-525.